INT. J. REMOTE SENSING, 1990, VOL. 11, NO. 2, 253-265

Geological features of the Spitsbergen region obtained from multispectral SPOT data and field radiometer measurements

N. LYBERIS, J. F. PARROT, J. CHOROWICZ and J. P. RUDANT

Université Paris VI, Département de Géotectonique,
4 Place Jussieu, 75252 Paris Cedex 05, France

(Received 19 July 1988; in final form 20 January 1989)

Abstract. In the Spitsbergen region (78°N), field radiometer measurements were collected from training zones considered to be representative of different lithological units and compared with the corresponding SPOT multispectral digital values. Correlations between field measurements and remotely-sensed data have been established, as well as the SPOT XS3 sensor's dependence on the solar zenith angle. On the basis of the relations between the field and satellite data, the boundaries between the different lithological units obtained from illuminated slopes can be extended into shaded zones.

1. Introduction

SPOT imagery has been tested in order to obtain geological data in arctic areas such as the Spitsbergen archipelago. The SPOT multispectral mode has three spectral bands (XS1, XS2 and XS3) in the visible and near-infrared wavelength ranges (0·50 to 0·59, 0·61 to 0·68 and 0·79 to 0·89 μm respectively).

In high latitudes (76°N to 80°N), the combination of Sun elevation and the mountainous morphology results in a large spread of shadow.

The albedo recorded by satellites depends on the atmospheric conditions as well as on the surface properties. In the present work we consider only the surface characteristics in comparison with geological data.

The spectral response of remotely-sensed data partly depends on the luminosity which is essentially a function of terrain slope, Sun azimuth and elevation angle (Holben and Justice 1980, 1981, Dave and Bernstein 1982, Kowalik and Marsh 1982), the presence of vegetation, colour and roughness of the ground all of which characterize the reflecting surface (Horwath 1981, Spiridonov *et al.* 1981, Escadafal and Pouget 1986). The colour and roughness factors of the ground response are strongly influenced by the vegetation cover, particularly when it is more than 30 per cent (Long *et al.* 1978, Graetz and Gentle 1982). It is important to point out that the Spitsbergen area is characterized by a lack of vegetation and the spectral response of the ground surface is therefore principally dependent upon the rock properties.

Considerable modelling efforts have been directed towards a better understanding of the effects of vegetation on the reflectance values (Stoner and Baumgardner 1981, Colwell 1981). In addition, the brightness of the ground depends upon the shadow created by its roughness (Girard 1983). In arid zones, which are comparable to the Spitsbergen region in lacking vegetation, the spectral luminosities in general depend on the characteristics of the ground surface, roughness (stoniness and soil crusting) and colour which are directly linked to the soil texture (Pouget *et al.* 1984).

Field measurements, taking into account the Sun elevation and azimuth, the slope

0143-1161 90 $3.00 © 1990 Taylor & Francis Ltd

angle, the roughness and the colour of the outcrops, have been made with a CIMEL portable radiometer calibrated with the SPOT satellite wavelength bands (CS1, CS2, CS3). The training zones were chosen on continuous slopes subjected to the same luminosity flux angle and relations between values calculated from field measurements and remotely-sensed data were obtained.

The results obtained on directly illuminated slopes have been extended to the shaded slopes, by using the method proposed by Mering and Parrot (1982). By this method geological boundaries can be recognized and from this it is possible to determine the structures affecting the rock units.

2. Field data

2.1. *Stratigraphy*

The investigated area is located on the southern edge of the Sassenfjorden fjord in central Spitsbergen (figure 1). The rocks in this area are mainly Mesozoic to Cenozoic sediments of shallow marine to non-marine origin (figure 2). The lithologic units of Triassic and Jurassic age are 1150 m thick. In this study only the Triassic to Jurassic sediments have been analysed.

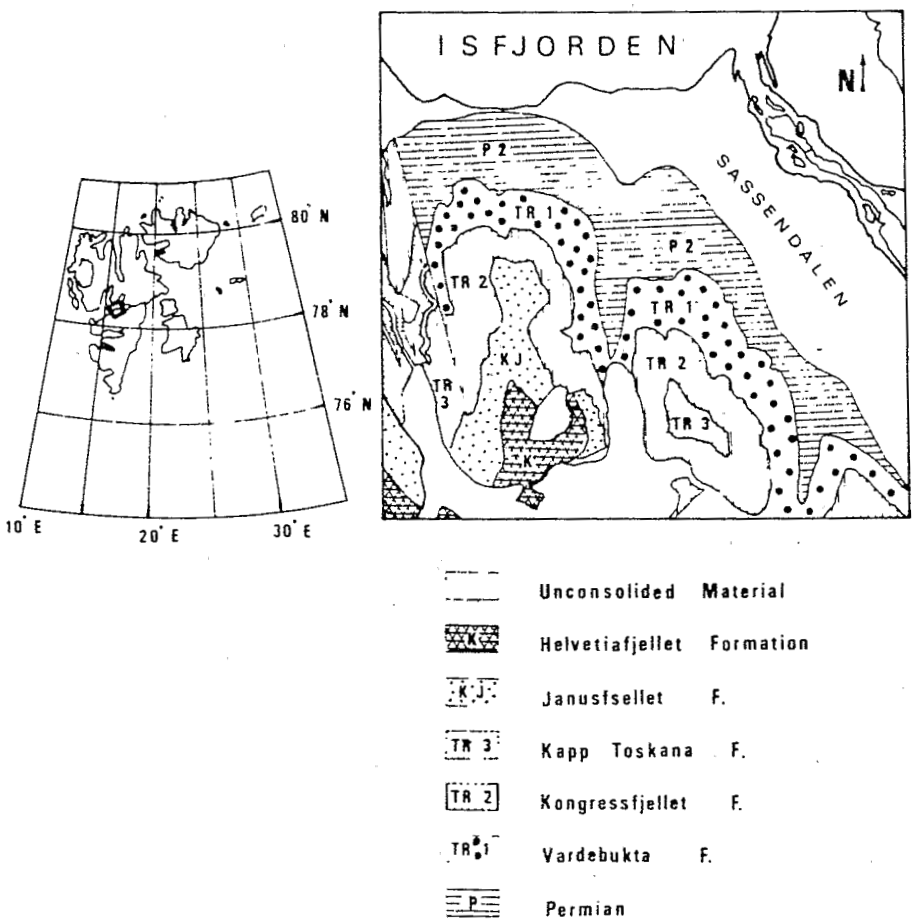

Figure 1. Geological map of the investigated area.

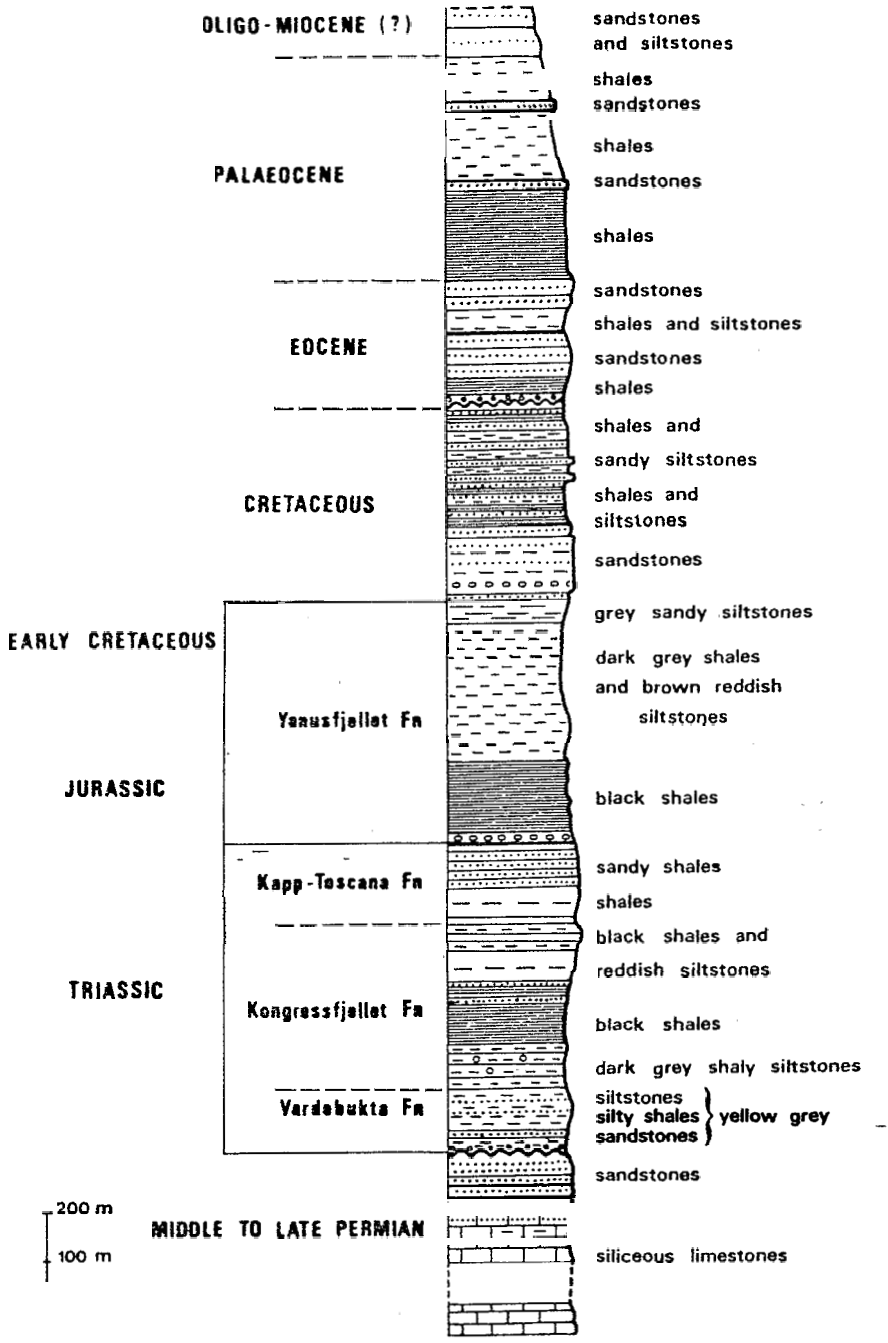

Figure 2. Stratigraphic column of the Marmierfjellet area sedimentary sequence.

The oldest layers are the deposits of the Lower Triassic Vardebukta Formation, consisting mainly of siltstones and silty shales with interbedded sandstones (Tozer and Parker 1968).

The Vardebukta Formation is overlain by the Kongressfjellet Formation belonging to the upper part of the Lower Triassic. The base of the Kongressfjellet Formation is composed of dark grey shales and shaley siltstones. The upper part of this formation is represented by dark and dark grey finely laminated shales with some interbedded siltstones. The dating of the 270 m upper part gives a Middle Triassic age (Tozer and Parker 1968).

The succeeding Kapp Toscana Formation is composed of dark grey shales and sandy shales of early Ladinian to Carnian age. Siltstones, sandy shales and sandstones located in the upper part of the sequence, are of Rhetian age (e.g. Major and Nagy 1972). The total thickness of the Kapp Toscana Formation is 250 m.

The overlying Janusfjellet Formation (Parker 1967), which is more than 500 m thick and corresponds to the Jurassic and Lower Cretaceous sequence, is composed of dark marine shales with lighter coloured sandstones. Siltstone beds are present in the upper part of this formation.

The lithological units described above are essentially horizontally bedded in the western Sassendalen area. Most of our training zones are located on the western slope of the Marmierfjellet, between the Sassendalen and Flowerdalen valleys (figure 1).

2.2 *Field measurements*

The training zones have been defined as representative of the different lithological units encountered. They are located on the satellite image in order to compare the field results and the satellite values.

For each training zone, several measurements were made in order to consider the different parameters of the ground surface. Parameters such as albedo, information about the structure and the texture of the ground surface, orientation of the site and the inclination of the slope have been taken into account. The constituent elements of the outcrops, and their proportions, have been measured. The recorded CIMEL values correspond to the ratio between the vertical component of the incident flux and the vertically reflected flux, measured on a 1 m^2 surface.

The training zones have been plotted on the corresponding satellite images. Each set of measures has been calibrated by comparison to a reference surface (baryte paper). Then the whole set of field measurements was restored on a homogeneous scale for the three SPOT bands. Thus, these calibrated values may be considered as results of measurements in comparable atmospheric conditions.

The field measurements take into account the colour of the outcrops as well as the presence of pebbles on the ground surface. The radiometric sampling areas were chosen to be more-or-less perpendicular to the flux luminosity angle; therefore, the effect due to the presence of pebbles on the reflecting surface is not significant. Thus, one can assume that the colour is the predominant parameter.

The different lithological layers consist of a mixture of shales, siltstones and sandstones. The stratigraphic levels differ from each other in the proportions of these three elements. As shown in figure 3, it is possible to discriminate the principal constituents of the stratigraphic column on the basis of the reflectance values in the three SPOT bands.

Figure 3 shows that the three wavebands strongly discriminate shales from sandstones. It is possible to distinguish the different types of shales in the third band,

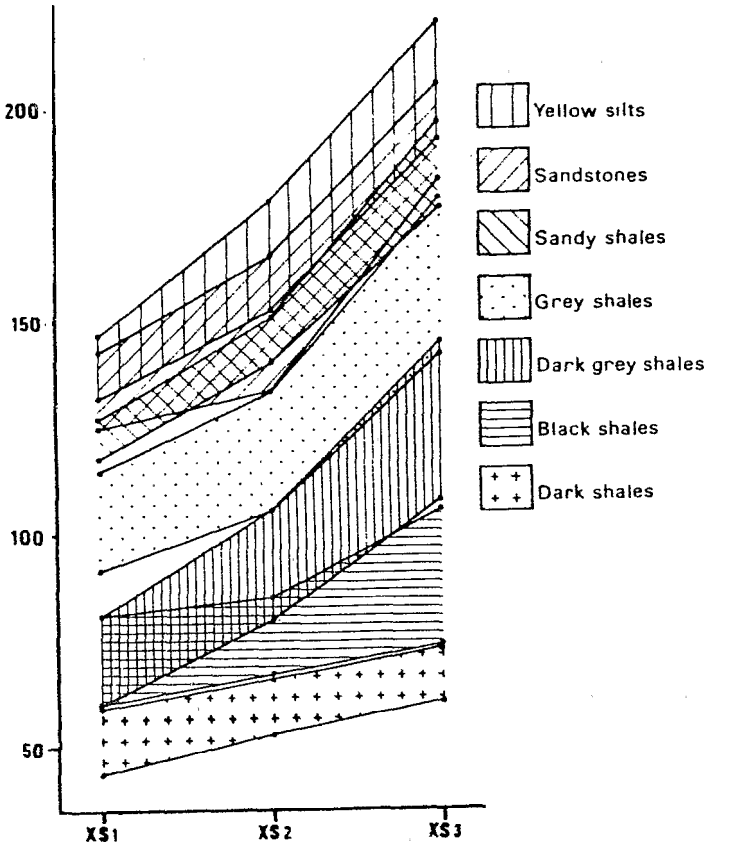

Figure 3. Diagram of the CIMEL radiometer measurements for the different lithological units.

CS3 (near-infrared). As for remotely-sensed data, the third waveband, CS3, is the best for discrimination.

3. Remotely-sensed data

The SPOT scene (path 157, row 141 on 27 August 1986 at 17.53.09 local time) was acquired when the maximum snow melting had occurred. At this time a significant area of outcrop is exposed, but unfortunately the Sun elevation is extremely low (7·5°), resulting in the development of shadowed zones hiding most of the landscape. In addition, the reflected light is very weak and the values for the illuminated rock formations are between 11 and 14 on XS1, between 8 and 11 on XS2 and between 5 and 14 on XS3. The corresponding reflectance values recorded on these three sensors were considerably decreased, especially in the XS3 band, because of the high moisture saturation on the surface of the lithological units due to the thawing action of frozen liquid within the rocks during the summer in Spitsbergen. On the other hand, as shown by Shine and Henderson-Sellers (1985), the albedo is drastically reduced at high latitudes where snow fields are abundant.

The remotely-sensed data encountered in the training zones located on illuminated slopes show that XS3 is better for discrimination than XS1 and XS2. The

SPOT values for shale outcrops (figure 3) are between 5 and 11 on XS3, whereas on XS1 they are approximately 11, and on XS2 between 8 and 9. The different types of shales (black, dark and grey) can be distinguished only by means of XS3. In contrast, the different types of sandstones can be distinguished on XS1 and XS2 bands. It is generally assumed that XS1 and XS2 cannot be correlated when vegetation is present. The correlation coefficients obtained for the outcrops on the satellite image, are XS1/XS2 = 0·8455, XS1/XS3 = 0·6920 and XS2/XS3 = 0·8207.

The following correlation coefficients are higher if we take into account the whole scene including snow and clouds, where they are XS1/XS2 = 0·9859, XS1/XS3 = 0·8869, and XS2/XS3 = 0·9331.

In both cases, the ratio of XS1 to XS3 shows the last degree of decorrelation. Therefore, we chose to use the bidimensional histogram XS1 versus XS3. However, relatively high values corresponding to the snow fields are scattered on this bidimensional histogram and it is possible to distinguish two different trends (figure 4). The first one lies in the 10 to 22 interval on XS1 and between 2 and 8 on XS3 and is related to ice fields and moisture, with low values in the near-infrared band. The second zone lies between 8 and 14 on XS1 and between 5 and 14 on XS3, and this corresponds to rocky surfaces. Thresholding the histogram surface corresponding to the rock units perpendicular to the main bisectrix and the lithological units can readily be identified (figure 5). In addition, analysis of the bidimensional histogram shows that the rock surfaces situated in shadow correspond to values between 8 and 10 on XS1, and between 5 and 8 on XS3 (figure 4).

4. Correlations between remotely-sensed data and field measurements

The collected CIMEL values are summarized in figure 3. Figures 6, 7 and 8 show the different trends of correlated CIMEL values versus SPOT values. The CIMEL values for each lithological unit are virtually linear (figures 6, 7 and 8). This feature is due to the weak range of the corresponding SPOT values whose scale has been stretched in order to illustrate the correlation, but the clustering effect has been eliminated.

The bidimensional histograms XS1/CS1 (figure 6) and XS3/CS3 (figure 8) show that, unlike the SPOT values, the CIMEL measurements discriminate between the different types of shales. On the other hand, yellow shales and sandstones which are discriminated between by the SPOT sensor, present the same CIMEL values. This difference seems to be due to the sampling. The yellow shales are often overlain by fragments of disrupted thin sandstone beds which are scattered on the ground surface. Measurements collected with the CIMEL radiometer on a 1 m^2 surface seem to correspond to a stoniness higher than that recorded by a SPOT pixel (400 m^2 surface). One SPOT pixel integrates the ensemble of the constituents (shales and fragments of sandstones).

Nevertheless, the correlation for each type of rock is linear on the bidimensional histogram XS2 versus CS2 (figure 7). The histogram XS3 versus CS3 (figure 8) is similar to the XS1 histogram except for the SPOT values for shales which are more stretched.

4.1. *Influence of the topographic effects*

The reflectance of the main lithological units is a function of the Sun elevation and azimuth (Rowan *et al.* 1977, Kowalik and Marsh 1982). The quantity of light received (E_{S1}) by a unit of ground surface depends on the Sun luminosity flux angle and is

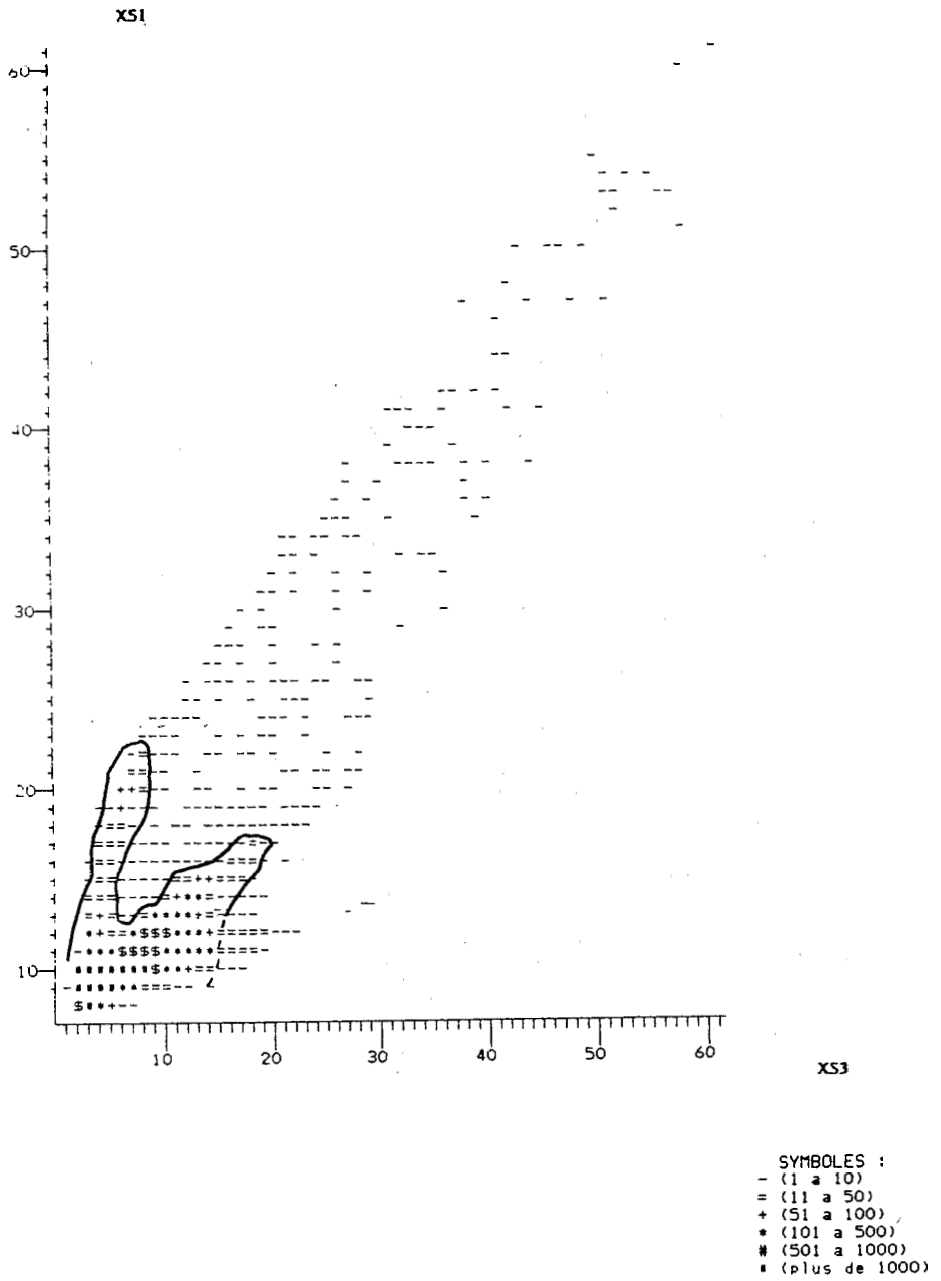

Figure 4. Bidimensional histogram, XS1 versus XS3, of the SPOT digital numbers in the studied area.

given by

$$E_{S1} = E_S \cos(NS)$$

where E_S = Sun illumination, N = normal to the ground surface and S = azimuth of the Sun.

Figure 5. Screen photography of the processed SPOT image (5·12 km × 5·12 km).

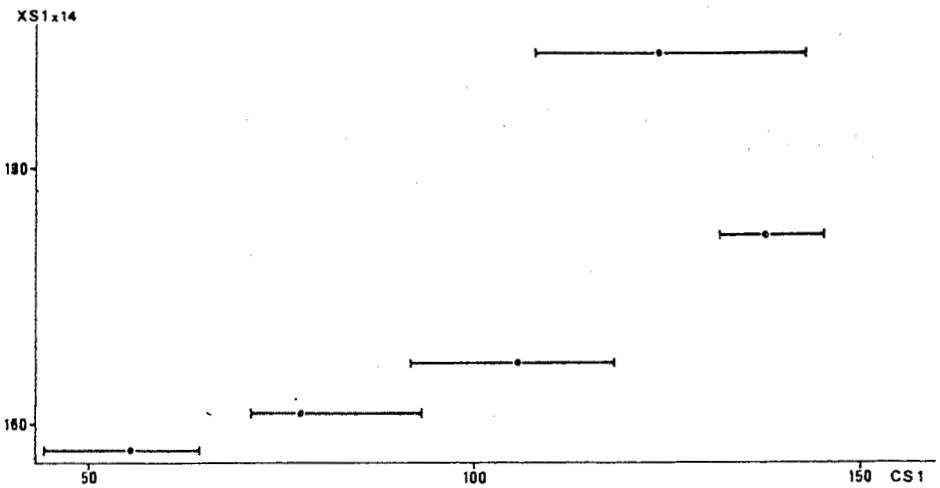

Figure 6. Diagram of the CIMEL values versus SPOT digital numbers for the lithological units of the training zones: XS1 versus CS1. The black circles correspond to the average values.

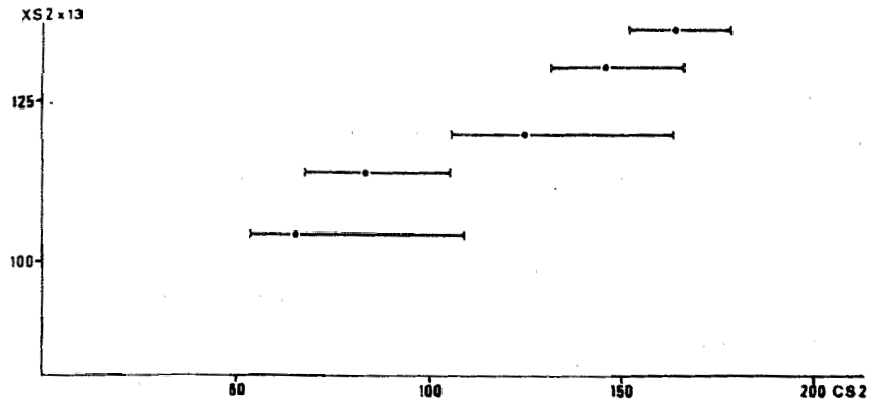

Figure 7. As figure 6 except for XS2 versus CS2.

If we consider in a first approach, horizontal surfaces and a Sun elevation of about 15° (mean value in August for the studied zone), the ground surface reflects only 25 per cent of the Sun luminosity flux. As a matter of fact, the highest value encountered on flat snow fields is about 64 on the SPOT reflectance recalibrated scale (0-255) at this date. The dip and strike of the slope have to be taken into account for the computation of the reflectance in the training zones.

The reflected flux (a) is computed as follows:

$$a = \cos\phi \sin(\phi + \theta)\cos\lambda \qquad (1)$$

where ϕ = dip angle (horizontal reference), θ = Sun elevation angle (horizontal reference) and λ = angle between solar azimuth and strike of the slope.

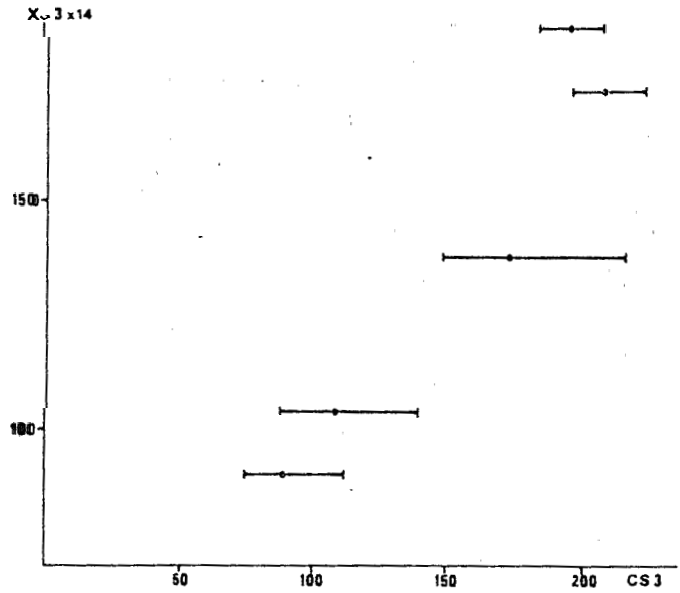

Figure 8. As figure 6 except for XS3 versus CS3.

Diagrams for the evolution of the a values were drawn for a 15° azimuth elevation angle, versus dip and strikes of the slope and different directions for the dip of the slope (figure 9). The value of the CIMEL degree (C_D) transposed to the SPOT reflectance scale can be computed as follows:

$$C_D = (256/T)KC_S a \tag{2}$$

where T = reflectance value of the reference target, K = factor depending on the used calibration target material and C_S = the direct CIMEL measurement.

The table shows a comparison between CD3 (values computed from CS3) and SPOT XS3 and a good correlation is observed even for the very low values registered in the satellite scene. XS1 and XS2 do not give such a good correlation, especially for the very low values. This result seems to be due to the diffuse illumination which is not computed in the present work. However, the atmospheric effects in SPOT XS1 are much more important than those from XS2 and XS3 bands (Singh and Cracknell 1986).

4.2. *Extension of the geological features into shady zones*

A close correlation is obtained in SPOT wavebands between rock units located on directly illuminated slopes and their spectral reflectance values in the Spitsbergen region where the scale of reflectance is very low. Measurements have been collected on all illuminated slopes in order to obtain similar conditions of analysis. The recorded measurements in shaded zones have been eliminated because of the extremely low scale of raw reflectance values on the SPOT data.

Shaded zones are common in the Spitsbergen area. They correspond either to indirectly illuminated slopes, or to shadows cast due to the very low Sun elevation.

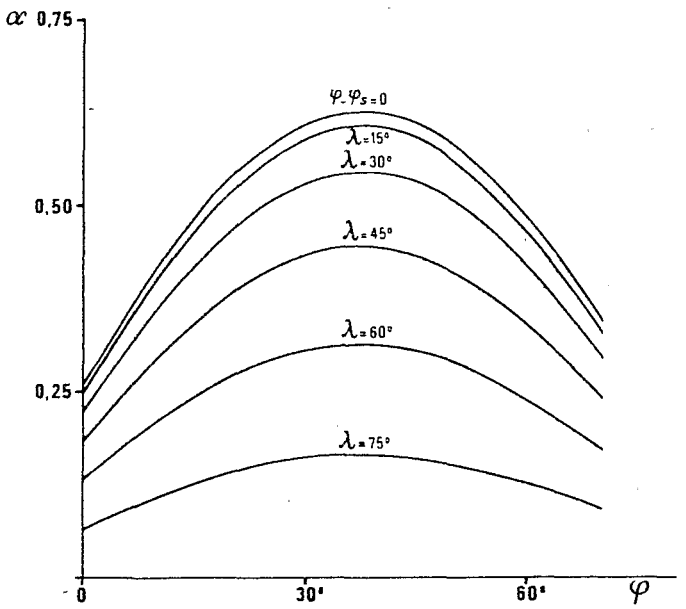

Figure 9. Diagram showing the evolution of the reflected flux (a) for different dips of the ground slope and different solar azimuths. The Sun elevation is 15°.

Comparison between the SPOT XS3 digital numbers, the field radiometer measurements (CS3) and the calculated values after correction for the topographic effect in the near-infrared band.

Lithology	Field data	Calculated values	SPOT values
Yellow silts	193–220	13·6	13–14
Sandstones	183–206	12·9	12–13
Sandy shales	179–197	12·12	11–12
Grey shales	143–176	10·8	9–11
Dark grey shales	108–145	8·2	8–9
Black shales	74–106	6·8	7–7
Dark shales	61–73	4·8	5–7

Lithological boundaries of mountainous regions recognized on sunlit slopes are more difficult to perceive on shaded slopes, because of the existence of high contrast between light and shadow.

Numerical methods such as the gradient mask or the Sobel mask (Pratt 1978) try to take this problem into account. They accentuate contrasts between all the homogeneous areas of different reflectance levels, but they only give a network of various directions along which structural trends (e.g. faults, bedding etc.) are filtered and are either accentuated or disappear.

The method proposed by Mering and Parrot (1982) is a mask which emphasizes the geological boundaries. The values of the ratio between successive pixels having effect in two adjacent lithological boundaries are computed so that they are similar in illuminated and shaded zones. The proposed function which selects the values is as follows: (*a*) if $I_D(K) \geq I_D(K+1)$

$$f[I_D(K), I_D(K+1)] = \frac{\log[I_D(K)+M_1]M_2}{\log[I_D(K+1)+M_1]} - M_2$$

(*b*) if $I_D(K) < I_D(K+1)$

$$f[I_D(K), I_D(K+1)] = 0 \qquad (3)$$

$I_D(K)$ and $I_D(K+1)$ correspond to the raw values of two successive pixels K and $K+1$. M_1 and M_2 are positive constants. M_1, generally equal to 20, allows the application of the logarithm function; M_2 equal to 500, improves the precision of the computation and places the result in the 0–255 field.

The different lithological units were identified first on the lightened areas. Then, by using equation (3), it is possible to discriminate the boundaries of the successive lithological units on the basis of the difference in the reflectance values for two consecutive pixels, either on one column or on one line. Equation (3) also takes into account the low reflectance values of the areas blanketed by shadows. The difference of reflectance values in the shady zones were enhanced to the same level as that of the illuminated lithological counterpart.

The use of this method makes it possible to delineate and determine the boundaries between the lithological units in areas covered by shadows utilizing parameters obtained from the lightened zones. Figure 10 illustrates the result of a thresholding of the images obtained by applying equation (3) to the XS3 SPOT band. On the processed document, the limits of the different rock units appear in the

Figure 10. Screen photography of the same SPOT image as in figure 5, processed using equation (3) (explanation in the text). The dotted lines correspond to the bedding.

lightened area as well as in the shady zones. In the raw image (figure 5), the central portion of the prints represents the shady zone, while the upper left-hand and the lower right-hand corners represent the lightened areas. Figure 10 shows a set of parallel dotted lines, trending NW–SE and NE–SW which indicates the bedding traces of the sandstones, sandy shales and shales.

5. Conclusions

SPOT multispectral records for rock outcrops situated in high latitudes (78°N) can be used for geological investigations, although the digital numbers are extremely weak because of the low Sun elevation angle. Radiometric measurements on the three SPOT wavebands collected under similar light conditions discriminate between the different lithological sequences. Comparison between the field reflectance values and the SPOT records leads to a recognition of the spectral signatures of these sequences.

Topographic effects as well as the Sun position have to be taken into account to establish the close correlation existing between XS3 values and field measurements.

On the basis of the relations obtained for illuminated slopes, the boundaries of the different lithological units can be extended into shaded zones, in order to sketch out geological maps.

Acknowledgments

We thank Geoff Manby for helpful comments. Financial support for this research provided by the ATP Télédétection project of CNRS as well as by the

French-Norwegian Research Fondation. The fieldwork benefited from logistic support by Elf Petroleum Company and the Norsk Polarinstitutt.

References

COLWELL, J. E., 1981, Landsat feature and enhancement, can we separate vegetation from soil? *Proceedings of the 15th International Symposium on Remote Sensing of Environment held in October 1981*, Vol. 2 (Ann Arbor, Michigan: Environmental Research Institute of Michigan), pp. 599–621.

DAVE, J. V., and BERNSTEIN, R., 1982, Effect of terrain orientation and solar position on satellite-level luminance observations. *Remote Sensing of Environment*, **12**, 331–348.

ESCADAFAL, R., and POUGET, M., 1986, Luminance spectrale et caractères de la surface des sols en région aride méditerranéenne (Sud tunisien). *ITC Journal*, **1**, 19–23.

GIRARD, M. C., 1983, Télédétection de la surface du sol. *Colloque INRA*, **32**, 177–193.

GRAETZ, R. D., and GENTLE, M. R., 1982, The relationships between reflectance characteristics in the Landsat wavebands and the composition and structure of an Australian semi-arid shrub rangeland. *Photogrammetric Engineering and Remote Sensing*, **48**, 1721–1730.

HOLBEN, B. N., and JUSTICE, C. O., 1980, The topographic effect on spectral response from Nadir-pointing sensors. *Photogrammetric Engineering and Remote Sensing*, **46**, 1191–1199.

HOLBEN, B, N, and JUSTICE, C. O., 1981, An examination of spectral band ratioing to reduce the topographic effect on remotely sensed data. *International Journal of Remote Sensing*, **2**, 115–133.

HORWATH, E. H., 1981, Spectral properties of Arizona soils and rangelands and their relationship to Landsat digital data. PhD Dissertation, University of Arizona, U.S.A.

KOWALIK, W. S., and MARSH, S. E., 1982, A relation between Landsat digital numbers, surface reflectance and the cosine of the solar zenith angle. *Remote Sensing of Environment*, **12**, 39–55.

LONG, G., DEBUSSCHE, G., LACAZE, B., LE FLOCH, E., and PONTANIER, R., 1978, Contribution à l'analyse écologique des zones arides de Tunisie avec l'aide des données de la Télédétection spatiale. Expérience Arzotu, Final report (1975–1978) CEPE. Louis Emberger, INRA-Tunisie, ORSTOM, CNES, Montpellier, France.

MAJOR, H., and NAGY, J., 1972, *Geology of the Adventalen map area*, No. 138 (Oslo: Norsk Polarinstitutt Skrifter).

MERING, C., and PARROT, J. F., 1982, Mise en évidence par analyse numérique des structures géologiques en zone montagneuse indépendamment des contrastes ombre-lumière. *Cahiers ORSTOM, Série Géologique*, **12**, 3–22.

PARKER, J. R., 1967, The Jurassic and Cretaceous sequence in Spitsbergen. *Geological Magazine*, **104**, 487–405.

POUGET, M., LORTIC, B., SOUISSI, A., ESCADAFAL, R., and MTIMET, A., 1984, Contribution of Landsat data to mapping of land resources in arid regions. *Proceedings of the 18th International Symposium of Remote Sensing of Environment held in Paris in October 1984*, Vol. 3 (Ann Arbor, Michigan: Environmental Research Institute of Michigan), pp. 1717–1728.

PRATT, W. K., 1978, *Digital Image Processing* (New York: Wiley & Sons).

ROWAN, L. C., GOETZ, A. F., and ASHLEY, R. P., 1977, Discrimination of hydrothermally altered and unaltered rocks in visible and near infrared multispectral images. *Geophysics*, **42**, 522–535.

SHINE, K. P., and HENDERSON-SELLERS, A., 1985, The influence of satellite spectral sensor response on the analysis of satellite imagery at high latitudes. *International Journal of Remote Sensing*, **6**, 29–34.

SINGH, S. M., and CRACKNELL, A. P., 1986, The estimation of atmospheric effects for SPOT using AVHRR channel-1 data. *International Journal of Remote Sensing*, **7**, 361–377.

SPIRIDINOV, H., KUNCHEVA, R., and MISHEVA, E., 1981, Results and conclusions from soil and vegetation reflection coefficient measurements. *Advances in Space Research*, **1**, 111–114.

STONER, E. R., and BAUMGARDNER, M. F., 1981, Characteristic variations in reflectance of surface soils. *Soil Science Society of America Journal*, **45**, 1161–1165.

TOZER, E. T., and PARKER, J. R., 1968, Notes on the Triasic biostratigraphy of Svalbard. *Geological Magazine*, **105**, 526–542.